Phonon Bottleneck in Graphene-Based Josephson Junctions at Millikelvin Temperatures

I. V. Borzenets, U. C. Coskun, H. T. Mebrahtu, Yu. V. Bomze, A. I. Smirnov, and G. Finkelstein

Phys. Rev. Lett. **111**, 027001 — Published 9 July 2013

DOI: 10.1103/PhysRevLett.111.027001

Phonon bottleneck in graphene-based Josephson junctions at millikelvin temperatures

I.V. Borzenets,[1] U.C. Coskun,[1] H.T. Mebrahtu,[1] Yu.V. Bomze,[1] A.I. Smirnov,[2] and G. Finkelstein[1]
[1]*Department of Physics, Duke University, Durham, NC 27708 and*
[2]*Department of Chemistry, North Carolina State University, Raleigh, NC 27695*

We examine the nature of the transitions between the normal and superconducting branches in superconductor-graphene-superconductor Josephson junctions. We attribute the hysteresis between the switching (superconducting to normal) and retrapping (normal to superconducting) transitions to electron overheating. In particular, we demonstrate that the retrapping current corresponds to the critical current at an elevated temperature, where the heating is caused by the retrapping current itself. The superconducting gap in the leads suppresses the hot electron outflow, allowing us to further study electron thermalization by phonons at low temperatures ($T \lesssim 1$K). The relationship between the applied power and the electron temperature was found to be $P \propto T^3$, which we argue is consistent with cooling due to electron-phonon interactions.

PACS numbers: 74.45.+c, 72.80.Vp, 63.22.Rc, 65.80.Ck

The electron-phonon interaction and the thermal properties of graphene have attracted a lot of attention (for an extensive review, see *e.g.* Ref. 1.) Most studies focused on relatively high temperatures; however, in the past year several experiments were performed at temperatures below 10 Kelvin[2–7]. Measuring the intrinsic thermal properties of graphene becomes more challenging in this regime. In particular, making normal metal contacts to graphene would provide the dominant thermalization path, effectively shunting the electron cooling by phonons[7]. In order isolate the phonon contribution to thermal transport in graphene below 1K, we have contacted the graphene crystal with electrodes made from lead (Pb), which becomes superconducting below $T \sim 7$K. Superconducting leads exponentially suppress the thermal transport of hot electrons outside of the sample, allowing one to study thermalization by phonons.

We study several superconductor-graphene-superconductor (SGS) junctions made on the same graphene crystal. Despite the fact that our junctions are overdamped[8], we observe that hysteresis exists between the switching current I_S (from the superconducting to the normal state) and the retrapping current I_R (from the normal to the superconducting state). To identify the origin of the hysteresis, we monitor I_S and I_R in one junction, simultaneously applying Joule heating at a different junction on the same crystal. By varying the heating power, we can prove that the hysteresis is caused by electron overheating[9,10]. Furthermore, by changing the pairs of contacts where heating is applied and where the critical current is measured, we conclude that electrons in graphene maintain a uniform temperature across the crystal, which could be significantly higher than the temperature of the substrate. Finally, since the switching current I_S is reproducible upon repeated current sweeps, we can use this quantity as a thermometer measuring the electron temperature. We can therefore monitor the electron temperature as a function of applied power, which allows us to estimate the electron-phonon scattering rate in graphene at sub-Kelvin temperatures.

Graphene was deposited on the Si/SiO_2 substrate using the standard mechanical exfoliation recipe[11] and verified to be a single layer by Raman spectroscopy[12]. Six parallel superconducting strips (500 nm wide) were deposited on top of the graphene crystal by thermally evaporating a 4 nm contact layer of palladium (Pd) followed by 120 nm of lead (Pb)[13]. Thereby, a total of 5 superconductor-graphene-superconductor (SGS) junctions were created with lengths of 0.3, 0.7, 1, 1.5 and 2 μm, labeled 1 through 5, respectively (Fig. 1a, b). The widths were roughly similar for all the junctions at around $\sim 5\mu$m. In order to measure the relatively small superconducting currents, the sample was encased in a copper box and cooled down to the base temperature of 35 mK. The wires connecting the sample to the measurement setup were filtered by cold RC filters and lossy coaxial cables.

Because of the low melting temperature of lead (Pb), graphene was not annealed prior to the measurements, causing the Dirac point to be shifted to $V_{gate} = -45$ V (see Fig. 1d inset) and the estimated mobility to be $\sim 500 cm^2/Vs$. (The exact mobility is difficult to calculate due to sample geometry and unknown contact resistance) . At the most open gate voltage which we used, $V_{gate} = +40$ V, the switching currents from the superconducting to normal state were $I_S \sim 40$ nA, ~ 20 nA, and ~ 5 nA for junctions $1-3$ respectively. The two longest junctions (junctions 4 and 5) never developed a supercurrent. These values are suppressed compared to the naive estimates of the critical current $I_C \sim \Delta/R_N e$ (R_N is the normal resistance of the junction) most likely due to disorder, as discussed in our earlier publication[13].

Nanoscale hybrid Josephson junctions tend to be underdamped due to the large capacitance shunting the junction's bonding pads to the back gate, resulting in a low plasma frequency[8] and reduced dissipation. To ensure that our junctions are overdamped, we made the leads connecting the pads to the junctions somewhat resistive (a few hundreds of Ohms). This resistance partially isolates the junctions from the pad capacitance and introduces additional dissipation[14]. Calculating the qual-

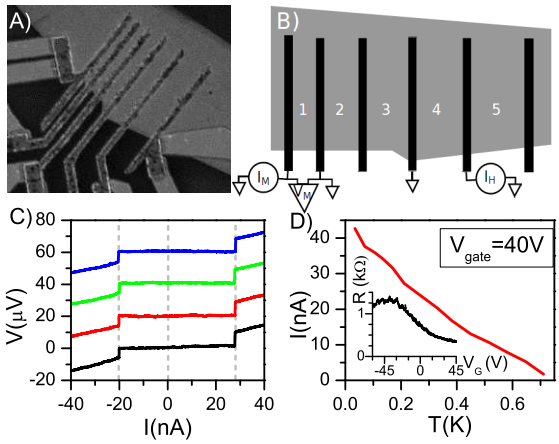

FIG. 1. a) Scanning Electron Micrograph of the sample. A layer of graphene (light-colored region at the top of the image) is contacted by superconducting electrodes (dark vertical stripes) made from Pd/Pb bilayer (partially oxidized following the measurements). Six contacts form five Josephson junction of different lengths (distances between the contacts). The superconducting electrodes extend just past one of the sides of the graphene crystal, where they are contacted by the normal metal electrodes. On their other end, the superconducting electrodes do not completely cross the crystal, allowing a thermalization path to connect the different regions of graphene. b) Schematic of the measurement setup for Figure 2. Differential resistance of one junction is measured, while a heating current I_H is applied to a different junction. c) Successive current sweeps (negative to positive) of junction 1 at V_{gate}=34 V showing reproducible values of I_S and I_R. d) Temperature dependence of I_S in junction 1 at V_{gate}=40 V. The temperature is set by heating the whole sample holder via an external heater. We use the switching current I_S as a sensor of the electron temperature later in the paper. Inset: The normal resistance R_N of junction 1 v.s. gate voltage V_{gate}.

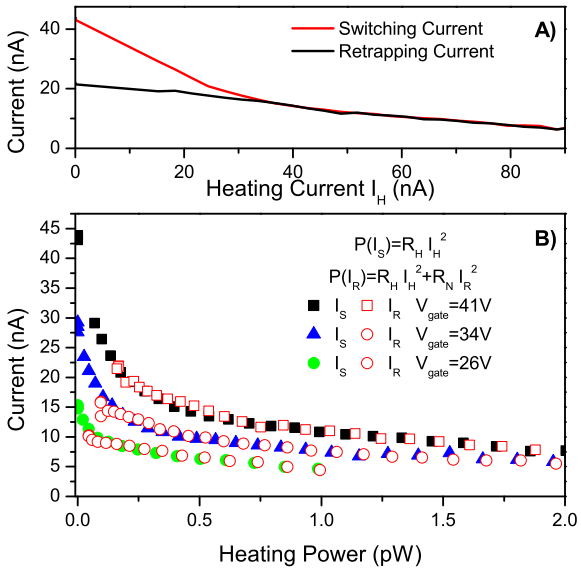

FIG. 2. a) The switching and the retrapping currents of the shortest junction (#1) versus the heating current applied to the longest junction (#5). The difference between the switching and the retrapping current disappears as more heating power is applied. b) Switching and retrapping currents versus the total heating power at different gate voltages. Since the retrapping current is necessarily measured while the junction is in the normal state, the power dissipated in that junction contributes to the total heating power. With this additional heating taken into account, the switching and the retrapping currents fall on top of each other. We conclude that the hysteresis between the switching and retrapping currents is caused by the self heating of the junction[9,10].

ity factor of the first junction, we find that it is overdamped for $I_C \gtrsim 10$ nA. (Here, we used the geometric pad capacitance $C_{pad} \approx 4$ pF, the lead resistance $R_{leads} \approx 300\ \Omega$ connected in series with the junction and the normal resistance $R_N \approx 450\ \Omega$ connected in parallel.)

As a result of the overdamping, successive current sweeps yield reproducible values of I_S (Figure 1c), allowing us to use the switching current as a measure of the electron temperature later in the paper (Figure 1d). However, the observed difference between the switching and retrapping current may appear to contradict the overdamped dynamics of the junction. In order to investigate the nature of this hysteresis, the graphene flake was heated locally by sending a current I_H through one of the five junctions, while measuring the critical current of another junction[2]. For example, junction 1 would be measured while the heating current I_H is sent through junction 5 (Figure 2a).

While the switching current I_S is reached when the measured junction is in the superconducting state, the retrapping current I_R is realized when the measured junction is in the normal state. Therefore, at the retrapping transition, additional power $P_R = R_N I_R^2$ is applied to graphene. Taking into account this additional power, we plot $I_S(P_H)$ and $I_R(P_H + P_R)$ in Figure 2b. (Here, $P_H = R_H I_H^2$ is the power applied at the heater junction[15].) I_S and I_R clearly fall on the same curve, demonstrating that at the same total dissipated power, I_S and I_R coincide.

The curves of I_S and I_R versus P map onto each other regardless of the junction that was measured (junctions 1 or 2) and for different gate voltages applied to graphene. Therefore, we can conclude that the retrapping current is suppressed compared to the switching current due to the heat dissipated by the retrapping current itself; the hysteresis between the switching and retrapping currents is thus due to the self-heating of the measured junction. Indeed, self-heating has been previously identified as the origin of the hysteretic behavior in overdamped SNS junctions made from metals[9,10].

Another conclusion that we draw from Figure 2 is that

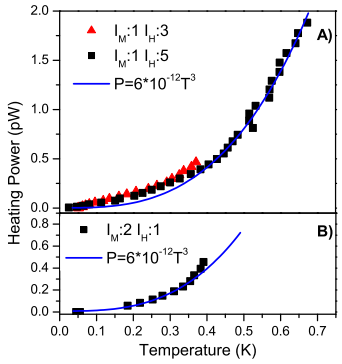

FIG. 3. Dissipated power *vs.* electron temperature in graphene. The latter was extracted by matching the switching current at a given heating current to the switching current measured by heating the whole sample. The graph presents three measurement configurations: a) measuring the switching current of junction 1 while heating junction 3 or junction 5, and b) measuring junction 2 while heating junction 1. The data for all three configurations fit well to a $P \propto T^3$ power law dependence with less than 5% difference in the proportionality factor, meaning that the electrons in the entire region are thermalized.

independently of the location at which the heating is applied – the heater junction or the measured junction – the total power spreads efficiently across the whole crystal. This means that electrons within graphene are well thermalized, allowing us to characterize the electron cooling in graphene in the remainder of the paper.

Instead of heating the graphene crystal locally by the current I_H, we can heat the entire sample (Figure 1d). We measure the switching current I_S in the two shortest junctions versus temperature T at several different gate voltages. By comparing the I_S *vs.* T data with the I_S *vs.* P data, we are able to extract the temperature up to which the electrons in the measured junction are heated for a given P. This way, a plot of P *vs.* T has been extracted for measured junction 1 while heating either junction 3 or 5 (Figure 3a). Similarly, in Fig. 3b, we measured junction 2 while heating junction 1. (In the latter case, large enough current was passed through junction 1 to overcome its own supercurrent. Once that happens, graphene heats to about 200 mK, which explains the gap in the data at lower temperatures.)

The three curves in Figure 3 are remarkably close, although the three setups have different distances and configurations of the heater and the measured junctions, implying that the entire region of graphene crystal in the vicinity of the junctions is thermalized to a uniform electron temperature. Empirically, the curves can be fitted by the same power law $P = 6 \cdot 10^{-12} \frac{\mathrm{W}}{\mathrm{K}^3}\ T^3$. This dependence rules out cooling by the hot electron diffusion into the superconducting leads. Indeed, the dependence would be exponentially suppressed in temperature due to the gap in the quasiparticle density of states of the

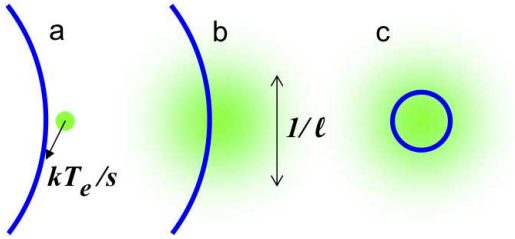

FIG. 4. Schematics. The blue line corresponds to the Fermi surface, the hot electron is shown in green. a) Clean case. A hot electron emits a phonon with a wave vector of $k_B T_e/hs$. b) Our case: phonon's wave vector is replaced by $1/l$. c) In the supercollision case[19], the wave vector uncertainty exceeds k_F.

superconductor. Even at T =1 K, the dissipated power ($6 \cdot 10^{-12}$ W) is several orders of magnitude larger than that estimated from the Wiedemann-Franz law, properly adjusted for the suppressed density of states in the leads ($\sim 10^{-16}$ W). This situation is different from the regime realized in Ref. 2, where a relatively small superconducting gap in Al leads allows them to provide a dominant thermalization path. We conclude that in our sample electrons in the graphene crystal are thermally decoupled from the leads and must be cooled by phonons.

Furthermore, the observed $P(T)$ cannot be limited by the Kapitza resistance between graphene and the substrate, which is estimated to be a few orders of magnitude smaller. (As an upper limit for the resistance, we take the values measured at 40 K in Ref. 16 and extend the cooling power according to $\propto T^3$ or $\propto T^4$.) Hence, graphene lattice must be well thermalized with the substrate. We conclude that the bottleneck for cooling in our system is the weak thermal coupling between electrons and phonons in graphene.

Following the derivation of Ref. 17, we estimate the electron-phonon cooling power in graphene as $\frac{AD^2\sqrt{n}}{\hbar^3 \rho_m s^2 v_F^2 l}(k_B T_e)^3$. Here, A is the area of graphene, D is the deformation potential constant, n is the electron density, ρ_m is graphene mass density, s is the speed of sound, and T_e is the electron temperature. In this formula, we assumed that at low temperatures the wavelength of the emitted phonon $hs/k_B T_e \gtrsim 1\mu$m, which enters the scattering matrix element, should be replaced (Fig. 4b) by a shorter distance l (most likely, the electron mean free path, estimated to be $\sim$ 100 nm.) [We also took into account that Ref. 17 calculated the transport time while we are interested in the scattering time, because each phonon emission event typically results in the electron energy loss of the order of $k_B T_e$.]

Plugging in the numbers from Refs. 17 and 18, we estimate the cooling power at $P = 10^{-12} \frac{\mathrm{W}}{\mathrm{K}^3}\ T_e^3$, within an order of magnitude from the measured value. [This is a rather crude estimate, in part because we do not know how large is the thermalized area of graphene crystal, which extends beyond the immediate vicinity of the contacts, see Figure 1a. This area determines A, taken to

be $(10\mu\text{m})^2$ in this estimate.]

Recent measurements of Refs. 3 and 4 report cooling power for hot electron $P \propto T_e^4$, indicating that the emitted phonon wavelength hs/k_BT_e is not cut off (Fig. 4a), as we assumed above. The difference may stem both from the lower temperatures in our measurement and a more restricted sample geometry resulting in shorter l in our case. The cooling power of Ref. 4, extrapolated down to 1 K would yield 0.07 W/m^2, which in fact is close to our result for $A = (10\mu\text{m})^2$.

Finally, $P \propto T_e^3$ dependence due to supercollision cooling[19] has been just observed in Refs. 20 and 21. This regime is realized if the wave vector of the emitted phonon, k_BT_e/s, exceeds the electron Fermi wave vector k_F (Fig. 4c); the emission process is enabled by the disorder. While disorder is also crucial in our case, we work in the opposite temperature regime, $k_BT_e \ll sk_F$ (Fig. 4b), so that the theory of Ref. 19 cannot be directly applied.

In conclusion, we have shown that the difference between the switching and the retrapping currents in our graphene Josephson junctions is caused by electron overheating in the normal state. The superconducting contacts thermally isolate the graphene crystal from the leads, allowing us to measure the electron temperature rise for a given dissipation power, and hence the electron-phonon energy transfer rate. The observed power law dependence $P \propto T^3$ is consistent with theory of electron-phonon interactions in graphene and with other measurements. Due to small electron heat capacitance and their decoupling from phonons, this type of sample may be useful for detector applications[22].

The work was supported by the Division of Materials Sciences and Engineering, Office of Basic Energy Sciences, U.S. Department of Energy, under Awards DE-SC0002765 and DE-FG02-02ER15354.

[1] A. A. Balandin, Nature Materials, **19**, 569 (2011).

[2] J. Voutilainen, A. Fay, P. Häkkinen, J. K. Viljas, T. T. Heikkilä, and P. J. Hakonen, Phys. Rev. B **84**, 045419 (2011).

[3] A. C. Betz, F. Vialla, D. Brunel, C. Voisin, M. Picher, A. Cavanna, A. Madouri, G. Féve, J.-M. Berroir, B. Plaçais, and E. Pallecchi, Phys. Rev. Lett. **109**, 056805 (2012).

[4] K. C. Fong and K. C. Schwab, Phys. Rev. X **2**, 031006 (2012).

[5] H. Vora, P. Kumaravadivel, B. Nielsen, and X. Du, Appl. Phys. Lett. **100**, 153507 (2012).

[6] J. Yan, M.-H. Kim, J. A. Elle, A. B. Sushkov, G. S. Jenkins, H. M. Milchberg, M. S. Fuhrer, and H. D. Drew, Nature Nanotech. **7**, 472 (2012).

[7] A. S. Price, S. M. Hornett, A. V. Shytov, E. Hendry, and D. W. Horsell, Phys. Rev. B **85**, 161411(2012).

[8] M. Tinkham, *Introduction To Superconductivity* (McGraw-Hill, 1996).

[9] H. Courtois, M. Meschke, J. T. Peltonen, and J. P. Pekola, Phys. Rev. Lett. **101**, 067002 (2008).

[10] P. Li, P. M. Wu, Y. V. Bomze, I. V. Borzenets, G. Finkelstein, A. M. Chang, Phys. Rev. Lett. **107** 137004 (2011) and Phys. Rev. B **84**, 184508 (2011).

[11] K. S. Novoselov, D. Jiang, F. Schedin, T.J. Booth, V. V. Khotkevich, S. V. Morozov, and A. K. Geim, PNAS **102**, 10451 (2005).

[12] A. C. Ferrari, J. C. Meyer, V. Scardaci, C. Casiraghi, M. Lazzeri, F. Mauri, S. Piscanec, D. Jiang, K. S. Novoselov, S. Roth, and A. K. Geim, Phys. Rev. Lett. **97** 187401, (2006).

[13] I. V. Borzenets, U. C. Coskun, S. J. Jones, and G. Finkelstein, Phys. Rev. Lett. **107**, 137005 (2011) and IEEE Trans. Appl. Supercond. **22**, 1800104 (2012).

[14] D. Vion, M. Götz, P. Joyez, D. Esteve, and M. H. Devoret, Phys. Rev. Lett., **77**,16, 3435, (1996).

[15] We used R_H as a fitting parameter to ensure the best match between the $I_S(P_H)$ and $I_R(P_H + P_R)$ curves. The resulting values of R_H are close to the measured two-probe resistances of the heater junctions. The difference between the two-probe resistance and R_H is explained by a more sophisticated set-up used in the heating measurement, where a fraction of the heating current can flow to several of the grounded contacts other than the designated heater ground. These parallel current paths reduce the effective resistance of the heater.

[16] Z. Chen, W. Jang, W. Bao, C. N. Lau, and C. Dames, Appl. Phys. Lett. **95**, 161910 (2009).

[17] E. H. Hwang and S. Das Sarma, Phys. Rev. B **77**, 115449 (2008).

[18] D. K. Efetov and P. Kim, Phys. Rev. Lett **105**, 256805 (2010).

[19] J. C. W. Song, M. Y. Reizer, and L. S. Levitov, Phys. Rev. Lett. **109**, 106602 (2012).

[20] A. C. Betz, S. H. Jhang, E. Pallecchi, R. Ferreira, G. Féve, J.-M. Berroir, and B. Plaçais, Nature Phys., **9**, 109 (2013).

[21] M. W. Graham, S.-F. Shi, D. C. Ralph, J. Park, and P. L. McEuen, Nature Phys., **9**, 103 (2013).

[22] C.B. McKitterick, D.E. Prober, and B.S. Karasik, arXiv:1210.5495v3 (2012).